# Layered effects on soil displacement around a penetrometer

Pin-Qiang Mo[a,*], Alec M. Marshall[b], Hai-Sui Yu[c]

[a] *State Key Laboratory for GeoMechanics and Deep Underground Engineering, China University of Mining and Technology, China. E-mail: pinqiang.mo@cumt.edu.cn*
[b] *Faculty of Engineering, University of Nottingham, UK. E-mail: alec.marshall@nottingham.ac.uk*
[c] *School of Civil Engineering, University of Leeds, UK. E-mail: PVC.int@leeds.ac.uk*

**Abstract**

The interpretation of cone penetration test (CPT) data is important for the in-situ characterisation of soils. Interpretation of CPT data remains a predominately empirical process due to the lack of a rigorous model that can relate soil properties to penetrometer readings. Interpretation is especially difficult in layered soils, where penetrometer response can be affected by several horizons of soil with different properties. This paper aims to provide some insight into the mechanisms of soil displacement that occur as a penetrometer is pushed into layered soils. Data is presented from centrifuge modelling of probe penetration in layered soils in an axisymmetric container where soil deformation patterns around the probe can be measured. Results obtained from uniform soil tests are also presented to illustrate the effects of soil density and stress level (i.e. centrifuge acceleration). A large influence zone is found to relate to the higher penetration resistance obtained in a denser soil. Differing soil displacement patterns at low and high stresses are

*Corresponding author

related to the tendency of the soil to dilate, with the well-known consequence of a non-linear increase of penetration resistance with stress level. Layered soil tests show a clear difference of soil deformation patterns compared to uniform tests, especially for vertical displacements. The peak value of vertical displacement of the soil occurs at dense-over-loose interfaces, while a local minima occurs at loose-over-dense interfaces. Parameters are proposed to quantitatively evaluate the layered effects on soil deformations and a deformation mechanism is described for penetration in layered soils based on the transition of displacement profiles.

*Keywords:* cone penetration test, soil displacement, layered effect

## 1. Introduction

Cone penetration tests (CPT) are frequently used in geotechnical engineering for in-situ evaluations of soil properties and profiles. CPT data is also valuable for use within pile design methods and for the evaluation of soil liquefaction potential. The response of a CPT is very complex; it relates not only to the mechanical properties of the soil in which the probe tip is penetrating, but also the properties and proximity of nearby horizons of soil. As such, rigorous analysis of CPT data is very difficult and interpretation generally relies on empirical relationships for soil identification and classification (Sadrekarimi, 2016).

The CPT probe generates a complex deformation field as it penetrates into the soil. For plane-strain conditions, a comprehensive illustration of soil patterns around a flat-bottomed penetrometer was provided by White (2002) and White and Bolton (2004). The tests were conducted at 1-g (g = gravity) within a pressure chamber, and the results include streamlines of soil movement and stress profiles at the base of the penetrometer. The evolution of soil element deformation was illustrated and the reduction of stresses above the pile tip was related to cavity contraction caused by the densification of soil around the shaft. Mo (2014) reported results from axisymmetric elevated-g tests using a geotechnical centrifuge in which a half-cylindrical probe with a conical tip was pushed along a Perspex wall into both uniform and layered soil profiles. A resistance ratio was proposed in order to evaluate the transition curve of penetration resistance as the probe moved from one soil layer to another. A fully three-dimensional investigation was achieved by Paniagua et al. (2013) by using digital image correlation on x-ray micro tomography data. The authors were able to evaluate deformations around a fully-cylindrical penetrometer pushed into pressurised samples of silt. Failure patterns were described from the evolution of volumetric and shear strains.

Natural soil deposits often consist of layers with varying thickness and mechanical properties. Gui and Bolton (1998) reported that the CPT profile in layered soils deviates from a uniform soil profile when the probe reaches a certain distance from the soil layer interface and that some distance is required to develop a new tip resistance once the probe has penetrated into the second soil layer. Thus the transition zone around the soil layer interface can be separated into two parts: (1) the transition zone above the interface in which the probe begins to sense the underlining soil layer, and (2) the transition zone below the interface which extends to the depth where the probe is no longer influenced by the upper soil layer. Transition zones around soil layer interfaces have been shown to depend on the properties and thickness of soil layers (Meyerhof and Sastry, 1978a,b; Youd and Idriss, 2001; Mo et al., 2015). Analytical methods (e.g. Vreugdenhil et al., 1994; Mo et al., 2017) and numerical approaches (e.g. Ahmadi and Robertson, 2005; Xu, 2007; Walker and Yu, 2010) have also been performed to investigate penetration problems in layered soils. Despite these valuable contributions, there is still a limited amount of data available on penetration induced soil deformations within layered soils.

In this paper, data obtained from geotechnical centrifuge modelling of cone penetration tests in layered soils are included, with a particular emphasis on the illustration of soil deformations around the probe. The experimental equipment is the same as that presented in Mo et al. (2015); the penetrometer consisted of a half-cylindrical probe with a conical tip which was pushed into the soil at a Perspex wall in an axisymmetric container, thereby enabling the measurement of subsurface soil movements using digital image analysis. The paper first discusses the effect of soil density and stress level effect on deformation patterns. This is followed by a detailed illustration of the effect of soil layering on soil deformation patterns. The paper supplements the work presented in Mo et al. (2015) and Mo et al. (2017) in several ways: (1) additional results are presented that relate to the effects of stress condition; (2) the method for interpreting layered effects on soil displacements is elaborated; (3) profiles of displacements after penetration are presented which indicate different mechanisms for a loose-over-dense compared to a dense-over-loose configuration of soil layers; and (4) transition parameters of both horizontal and vertical displacements are introduced to quantitatively evaluate the layered effects on soil displacements, which are also related to the transitions based on penetration resistance.

## 2. Centrifuge tests and soil deformation measurement

Centrifuge tests were conducted using Fraction E silica sand (mean grain size $d_{50} = 0.14$ mm) with layers of varying relative density in a 180$^\circ$ axisymmetric model. Tests were performed on the Nottingham Centre for Geomechanics (NCG) 2 m radius geotechnical centrifuge. The penetrometer had a diameter of $B = 12$ mm and was pushed into the sand at a speed of 1 mm/s. Soil models were prepared by the multiple-sieving air pluviation method (Mo et al., 2015) to either a relatively dense state with relative density ($D_r$) of approximately 90 % or a relatively loose state with relative density of approximately 50 %. Note that the relatively loose sand, referred to simply as loose in this paper, falls within the 'medium dense' range ($D_r$ = 35 % $\sim$ 65 %), and the relatively dense sand, referred to as dense, falls within the 'very dense' range ($D_r$ = 85 % $\sim$ 100 %), based on $BS\,EN\,ISO\,14688-2:2004$. Tests were performed at both 50 $g$ (centrifuge acceleration) and 1 $g$ to evaluate the effects of stress level. Note that at prototype scale, the penetrometer represents a 0.6 $m$ diameter pile, which is comparable to a typical full-scale driven pile. The comparison between 50 $g$ and 1 $g$ results aims to provide an indication of the effect of stress condition on the induced soil deformation mechanism. Details of the layered soil profiles are summarised in Table 1.

A half-cylindrical model container with a Perspex window was used to enable the observation of penetration-induced sub-surface soil deformations, as shown in Figure 1(a). Digital cameras were used to obtain a series of images of the penetrometer and soil throughout the tests. Soil deformations caused

Table 1: Details of soil profiles for centrifuge tests

| Test ID | Soil Layer Details | Depth of Soil 1 (mm) | Depth of Soil 2 (mm) | Depth of Soil 3 (mm) | Total depth (mm) |
|---|---|---|---|---|---|
| T01-1g | D | 297 | - | - | 297 |
| T02 | D | 301 | - | - | 301 |
| T03 | L | 298 | - | - | 298 |
| T04 | L/D | 85 | 205 | - | 290 |
| T05 | D/L | 97 | 201 | - | 298 |
| T06 | L/D/L | 87 | 65 | 142 | 294 |
| T07 | D/L/D | 90 | 57 | 153 | 300 |

'D': dense sand ($D_r \approx 90$ %); 'L': loose sand ($D_r \approx 50$ %);
'L/D': loose over dense layers; Soil 1 is upper soil.

by the penetrometer, schematically presented in Figure 1(b), were measured using the Matlab-based image analysis methodology 'geoPIV' developed by White et al. (2003). Note that '$X$' and '$Y$' represent the horizontal and vertical positions of soil elements, and '$\Delta x$' and '$\Delta y$' indicate horizontal and vertical displacements, respectively. '$H$', defined as $H = z - z_{interface}$, indicates the distance between the cone shoulder and the soil layer interface. The upper soil layer interface is taken as the location of $z_{interface}$ (Figure 1b) to define $H$ for multi-layered tests. Further details on test set-up and procedures can be found in Mo (2014).

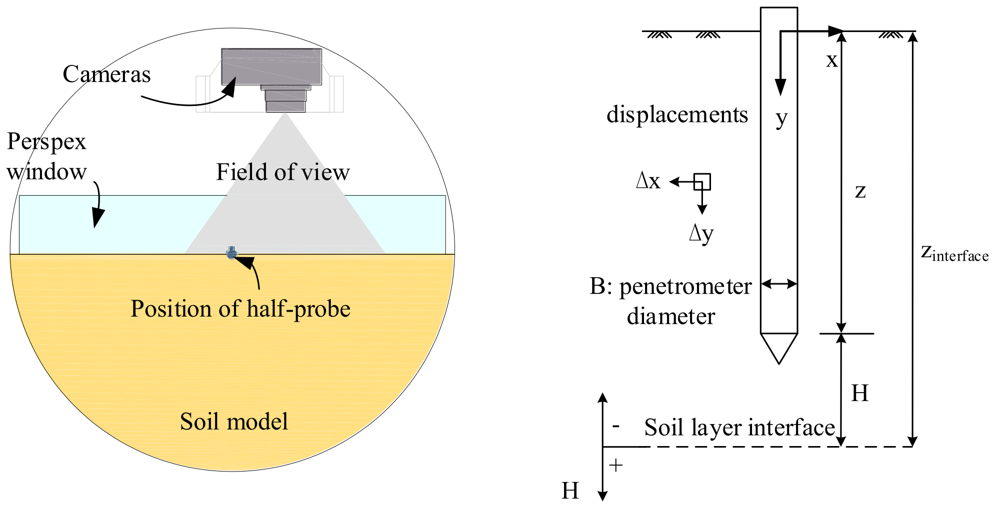


(a) Plan view of the centrifuge container (b) Schematic diagram of penetration test parameters

Figure 1: Centrifuge tests: (a) Plan view of the centrifuge container; (b) Schematic diagram of penetration test parameters

## 3. Results and Discussion

### *3.1. Effects of soil density*

It has been demonstrated that the response of a penetrometer in granular soils is dominated by two factors: confining stress and soil density (e.g. Lee, 1990; Bolton et al., 1999; Mo, 2014). In a granular soil, as the probe advances into the soil, the particles are pushed outwards to accommodate the probe and are simultaneously dragged downwards owing to shearing at the soil-probe interface. The soil around the probe is compressed and confining stresses in the soil increase, which in turn act on the probe and increase the penetration resistance. Results from the uniform soil tests T02 and T03 can be used to illustrate the effects that soil relative density and penetration depth have on deformation patterns. Figure 2 presents the profiles of normalised cumulative displacement $(2\,\Delta x/B, 2\,\Delta y/B)$ after 160 mm of penetration for soil elements located at varying normalised offsets $(2\,X/B = 2 \rightarrow 6)$ from the penetrometer in tests T02 and T03. The figure shows the relative radial ($\Delta y$ on the left-side of the plots) and axial ($\Delta x$ on the right-side) displacements that occurred within the soil. The deformation fields for the dense and loose tests are similar, though deformations extend further away from the probe and surface heave ($-\Delta y$) is more obvious in the dense sand test. Additionally, strains calculated based on the soil displacement data showed that the loose sand close to the probe experienced larger volumetric strains owing to the greater compressibility and less restricted dilation (Mo, 2014).

The movement of a soil element near the probe is initially predominately downwards, but becomes increasingly outwards as the probe approaches, ultimately reaching a similar vertical and horizontal movement (White and Bolton, 2004; Liu, 2010; Mo et al., 2015). As a result, penetration leads to a cylindrical deformation zone around the probe shaft and a spherical deformation region ahead of the cone, as shown in the cumulative displacement profiles in Figures 2 and 3. For soil around the probe shaft, the reduction of displacement with offset from the penetrometer implies that the observable lateral influence zone is about $5\,B$ wide for dense sand, and approximately $3.5\,B$ for loose sand, based on the results from Mo et al. (2015). Note that this influence zone is defined based on the PIV displacement data (i.e. the zone where the PIV technique was able to measure displacements caused by penetration) and does not define the distance required to a boundary required to avoid boundary effects. For the same tests, the value of cone

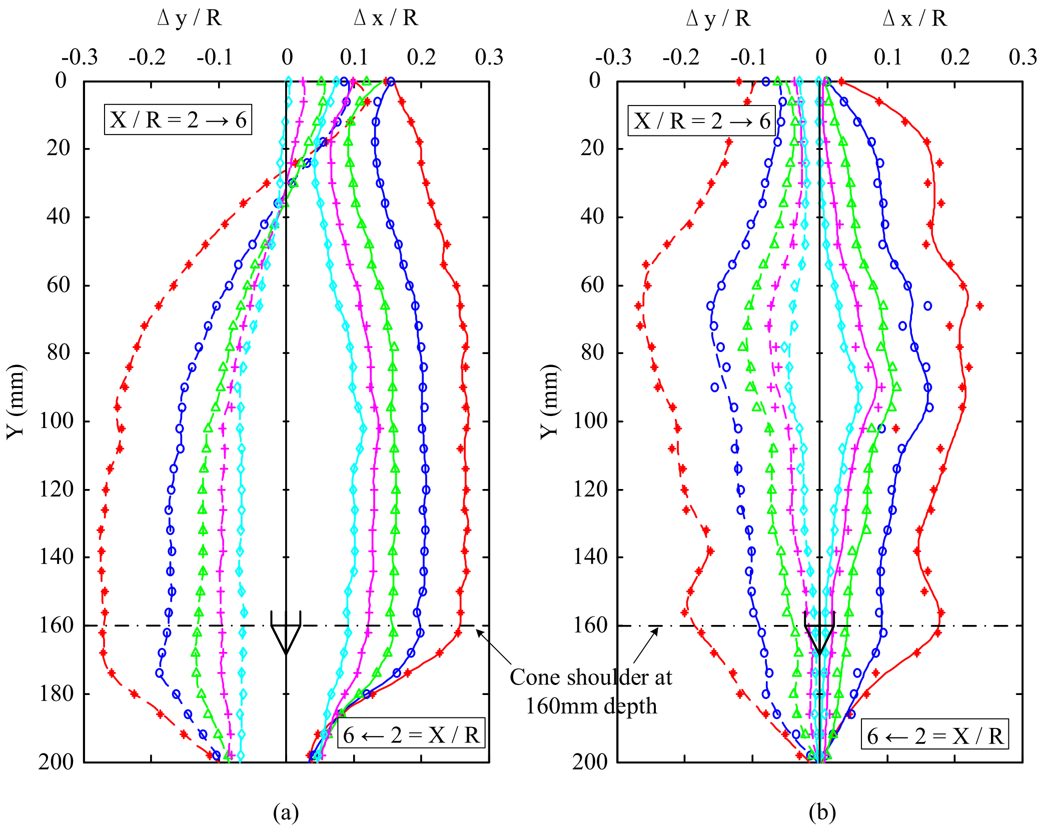


Figure 2: Cumulative displacement profiles after 160 mm of penetration: (a) dense sand: T02; (b) loose sand: T03

tip resistance in the dense sand was found to be about 2 − 3 times that for the loose sand. There is certainly a link between observed soil displacement patterns and penetration resistance, though this data indicates that it is not a simple linear relationship.

### *3.2. Effects of stress level*

The uniform dense sand tests at different g-levels (T01: 1 g and T02: 50 $g$) can be used to demonstrate the effects of stress level on data obtained from penetration tests. The magnitude of penetration resistance of the 50 g test was found to be $10 - 12$ times greater than that from the 1 g test (Mo, 2014), indicating that the penetration resistance does not scale linearly with g-level (as demonstrated by Bolton et al., 1999). In order to illustrate the effects of initial stress level (i.e. centrifuge acceleration) on soil deformations, Figure 3 provides contours of cumulative and instantaneous total displacements ($\sqrt{\Delta x^2 + \Delta y^2}$) for both the 50 g and 1 g tests. The total displacement after 120 mm of penetration from the 1 g test shows a slightly larger deformation zone as well as more pronounced heaving near the surface. Similar trends are also shown in the instantaneous contours ($\Delta z = 6$ mm in subplots (c) and (d) represents an interval of penetration distance), where the heaving effect in the 50 g test is more constrained by the higher stress levels.

From the results of the 1 g test, the larger deformation contours, especially for the soil near the surface, indicate the higher volumetric strains that are a consequence of the increased tendency of the soil to dilate under lower confining stresses (compared to the 50 g test). The instantaneous total displacement vectors also show that the soil is displaced more outwards and upwards in the 1 g test, indicating the dilatant behaviour induced by the shearing around the cone. The larger deformation zone in the 1 g test would therefore create a relatively higher stress state around the probe in the 1 g test compared to the 50 g test. Thus the ratio between the cone tip resistance and the in-situ stress condition ($q_c/p'_0$) would decrease as the stress level is increased (i.e. from the 1 g to 50 g test), which has been reported as a typical phenomenon for cone penetration tests from both field and laboratory trials (Jamiolkowski et al., 1988; Bolton et al., 1999).

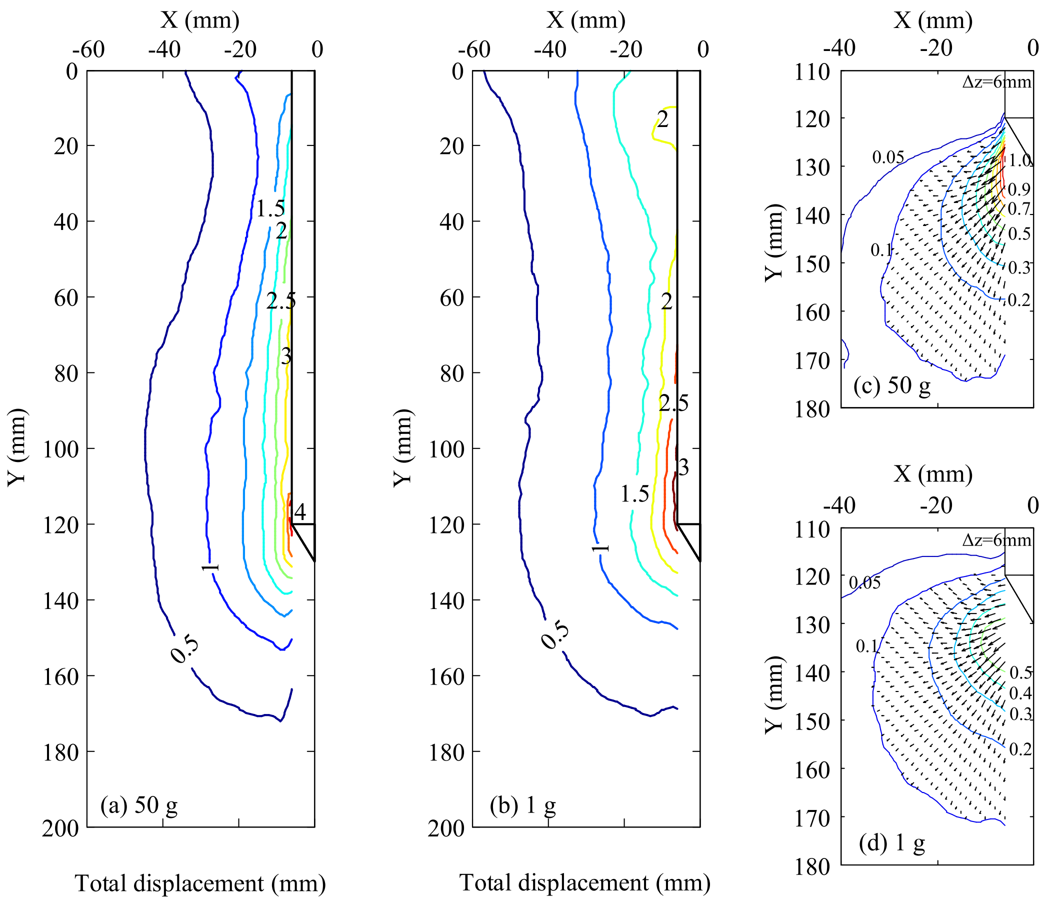


Figure 3: Contours of total displacements after 120 mm of penetration in dense sand: cumulative displacements (in mm): (a) 50 g, (b) 1 g; instantaneous displacements (in mm): (c) 50 g, (d) 1 g

### 3.3. Layered effects on soil displacements

This section considers the displacement data from the layered soil centrifuge tests. The transition of penetration resistance in two-layered soil tests is presented in Figure 4a. A cone tip resistance ratio $\eta'$ was defined by Mo (2014) as

$$\eta' = \frac{q_c - q_{c,w}}{q_{c,s} - q_{c,w}} \tag{1}$$

where $q_{c,w}$ and $q_{c,s}$ are the resistance in the uniform weak (loose) and strong (dense) soils, respectively. The trend of $\eta'$ tracks the transition of cone tip resistance $q_c$ when penetrating in layered soils and varies from 0 in a relatively weak soil layer to 1 in a relatively strong layer. The expression

$$\eta'_{fit} = \frac{1}{1 + S_1 \times exp(S_2 \times H/B)} \tag{2}$$

can be fitted to the $\eta'$ data from the two-layered tests in Figure 4a, where $H$ is the distance to the soil layer interface normalised by penetrometer diameter $B$ (Figure 1) and $S_1$, $S_2$ are curve fitting parameters. When the probe is pushed from loose into dense sand (T04), $\eta'$ transforms from 0 to 1, and the transition zone is larger in the dense layer ($4\,B$) compared to the loose sand ($2\,B$). For the tests where the probe goes from dense sand to loose sand (T05), the transition zone is again larger in the dense sand ($5\,B$) than in the loose sand ($1\,B$).

Figure 5 shows the profiles of normalised cumulative displacement in the two-layered tests (T04-T05), which illustrate a considerable curvature in the profiles of displacements around the location of the layer interface between the loose and dense soils. For the test with loose over dense sand (T04),

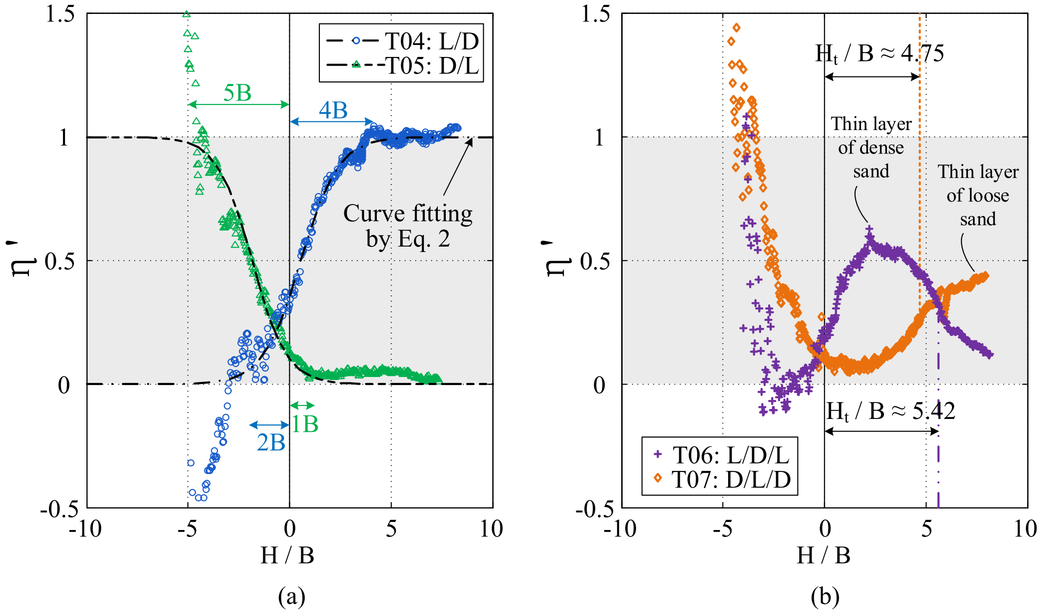


Figure 4: Layered effects on penetration resistance: (a) two-layered soils; (b) three-layered soils

the transition zone in the loose soil is around $2\,B$ based on the profile of $2\,\Delta y/B$, where the penetration resistance starts to be affected, as shown in Figure 4a. This agrees with the extent of the transition zone based on $\eta'$ in Figure 4a. A local minimum of $2\,\Delta y/B$ occurs at the loose-dense interface, followed by the gradual increase of vertical displacement as the probe pushes into the dense soil. The extent of the transition zone in the dense soil is not clear from this data. A slight increase of horizontal displacements occurs at the transition from loose to dense sand layer, however the transition zones around the layer interface are not clear based on the $\Delta x$ data.

For the test with dense over loose sand (T05), by comparing the data in Figure 5b with those in Figure 2a, it can be seen that the vertical displacements occurring when the probe approaches the layer interface are larger in the layered test compared to those at an equivalent depth in the uniform dense test. The peak displacement of $2\,\Delta y/B$ occurs at the dense-over-loose interface, and the transition zone in the loose sand is about $4\,B$ based on vertical displacements. This is much larger than the value of $1\,B$ observed from the resistance transition curve in Figure 4a. Again, there is a small change (decrease) of horizontal displacement from dense to loose sand layer, but this data can not be used to identify the extent of a transition zone.

Similar trends can also be found for tests T06 and T07 (Figure 6), where a thin layer of dense or loose sand is sandwiched between layers of loose or dense sand, respectively. The observation confirms that the peak value of vertical displacements occurs at the dense-over-loose interface, whereas a local minimum occurs at the loose-over-dense interface.

Figure 7 shows the locations (based on measured displacements) of the soil

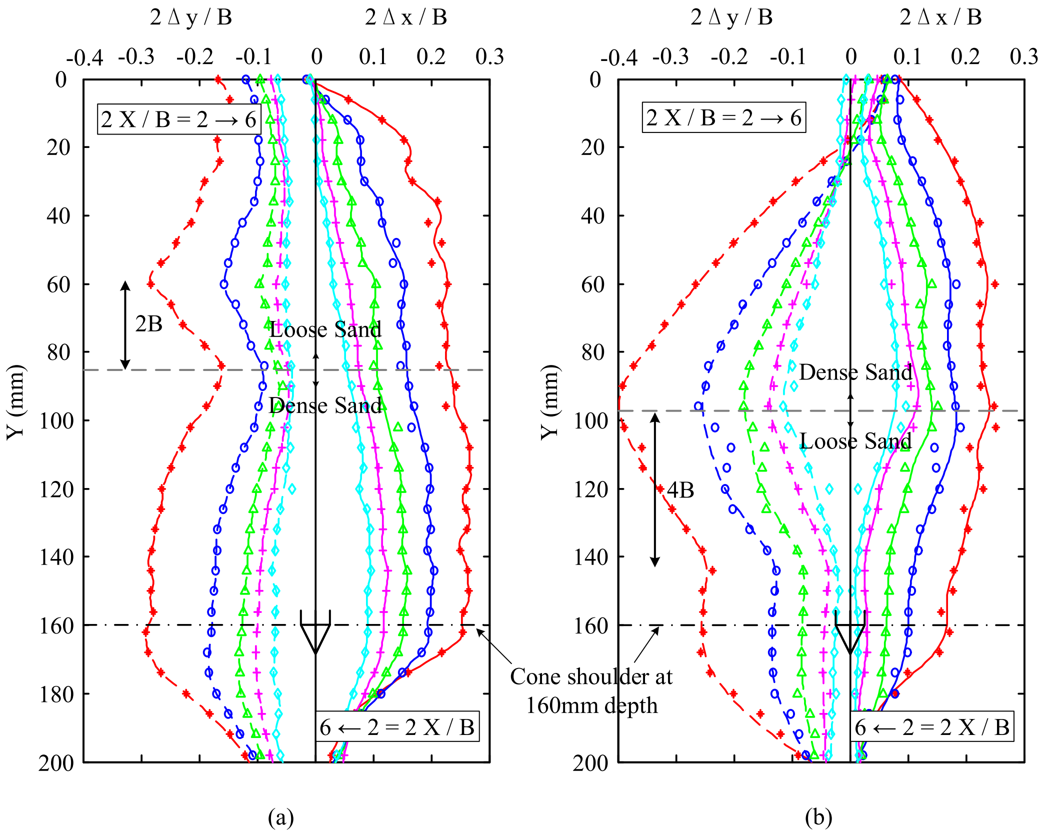


Figure 5: Cumulative displacement profiles after 160 mm of penetration: (a) loose over dense T04; (b) dense over loose T05

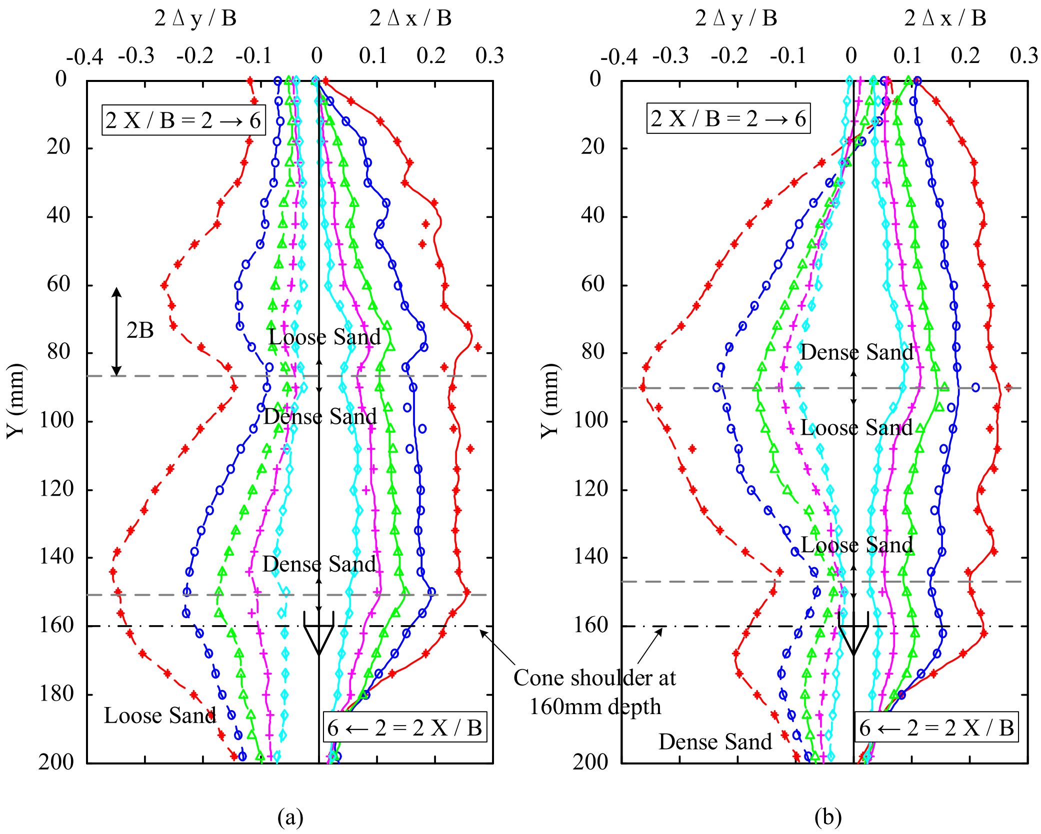


Figure 6: Cumulative displacement profiles after 160 mm of penetration: (a) dense sandwiched between loose T06; (b) loose sandwiched between dense T07

layer interface during the layered tests after 160 mm of penetration. Included in the plots are data from the uniform dense (T02) and loose (T03) tests based on displacements at depths corresponding to the locations of the interfaces in the layered tests. The displacements from the uniform tests are similar for the dense and loose sand at shallower depths ($Y$ =85 to 98 mm in plots a, b, c-1 and d-1) but differ slightly at deeper locations ($Y \approx 150$ mm in plots c-2 and d-2), where the dense sand experiences greater displacements.

The displacements from the layered tests are shown to fall outside of the range of displacements from the uniform sand tests. The displacements from the loose-over-dense interfaces are always less than the displacements from both the uniform dense and loose tests, supporting the observation of a local minimum at the layer interface in the $\Delta y$ data in Figures 5 and 6. The opposite is true for the dense-over-loose interfaces, where displacements are greater than those from both the uniform dense and loose tests (indicating a peak in $\Delta y$ observed at the layer interfaces in Figures 5 and 6).

The data presented thus far indicate that the pattern of soil displacements around the interfaces between soil layers is affected by the properties of the soil in the respective layers. However, the figures have not demonstrated a clear definition of the extent of the transition zones based on soil displacement data. In order to better quantify the extent of the transition zones from the displacement data, the approach adopted for penetration resistance (Xu and Lehane, 2008; Mo, 2014) is now applied to the displacement data.

Following the definition of the cone tip resistance ratio $\eta'$ in Equation 1 (plotted in Figure 4), the changes of soil deformation between layered and uniform tests can be treated as a ratio, which is termed $\xi'$. Due to the

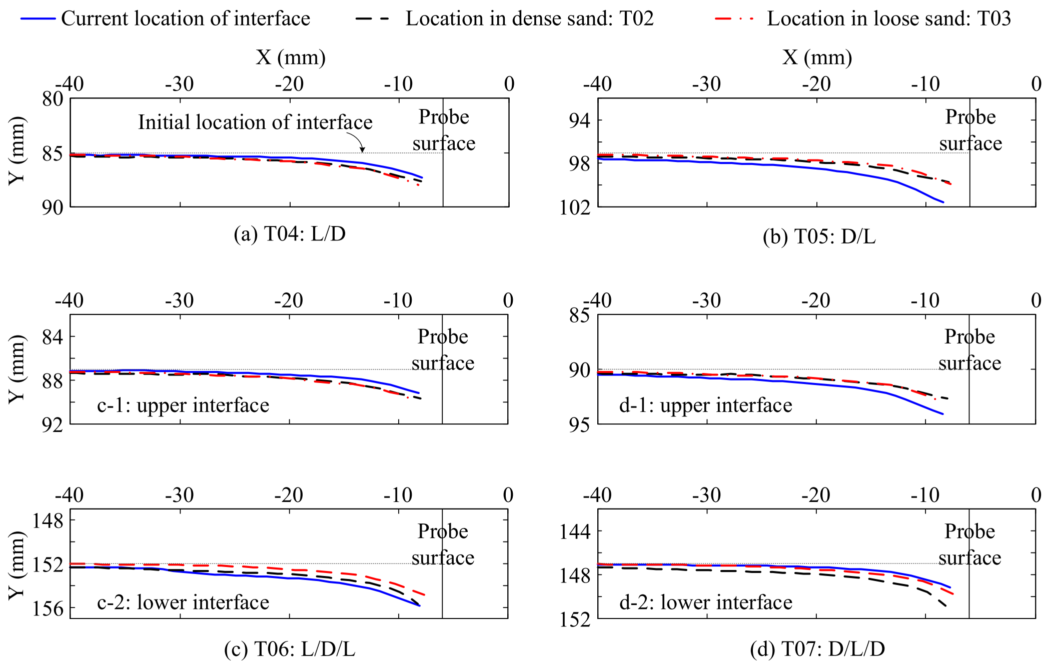


Figure 7: Displacement of soil layer interfaces after 160 mm of penetration for tests: T04-T07

different magnitude of the effect of soil layering on horizontal and vertical displacements, $\xi'$ is evaluated for $\Delta x$ and $\Delta y$ separately as:

$$\xi'_{\Delta x} = \frac{\Delta x - \Delta x\,|_w}{\Delta x\,|_s - \Delta x\,|_w} \tag{3}$$

$$\xi'_{\Delta y} = \frac{\Delta y - \Delta y\,|_w}{\Delta y\,|_s - \Delta y\,|_w} \tag{4}$$

where the subscripts ‘s’ and ‘w’ relate to the uniform soil tests with dense (strong) and loose (weak) sand, respectively.

Figure 8 considers test T04 in particular, where loose soil overlies dense soil. Calculation of $\xi'$ was based on the cumulative displacements ($\Delta x$ and $\Delta y$) after 160 mm of penetration. Displacements at an offset distance of $2\,X/B = 2$, illustrated in subplot (a), were used to calculate the values of $\xi'_{\Delta x}$ and $\xi'_{\Delta y}$ in subplots (b) and (c), respectively. The displacement data from the uniform dense and loose tests (T02 and T03), which are used in the calculation of $\xi'$, are also included in subplot (a).

Similar to the transition curve of $\eta'$ (see Figure 4a), the transition of $\xi'_{\Delta x}$ generally varies from 0 in the loose sand to 1 in the dense sand, as shown in Figure 8(b). The scatter in the $\xi'_{\Delta x}$ is rather large in the loose sand layer due to the fact that values of $\Delta x$ were very similar in all of the tests (see Figure 8(a)).

The value of $\xi'_{\Delta y}$ also transforms from 0 to 1, but values around the layer interface range widely beyond the $0 \rightarrow 1$ limits. These values occur because of the layered soil effect on the trend of $\Delta y$ in test T04 as well as the seemingly coincidental ‘crossing’ of the $\Delta y$ data from the uniform loose and dense tests near the location of the layer interface in test T04. The magnitude of $\xi'_{\Delta y}$

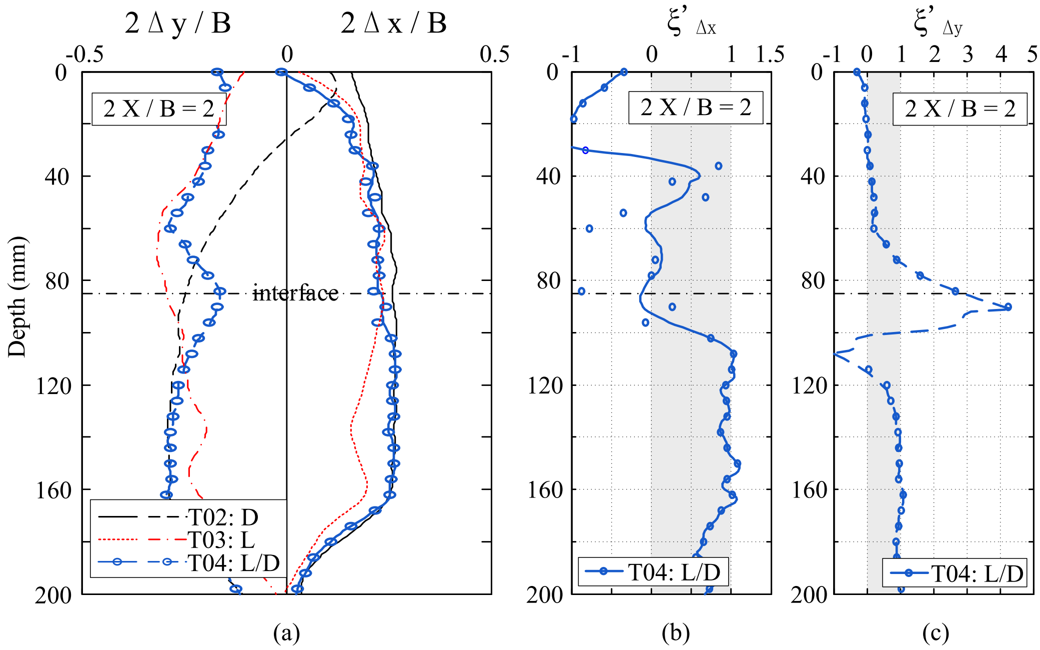


Figure 8: Layered effects on soil deformation ($2\,X/B = 2$) for test T04

increases up to approximately 4 in the soil just below the layer interface and drops dramatically to negative values at $H/B \approx 2$. Below this location, $\xi'_{\Delta y}$ increases gradually to 1 as the displacements in the layered tests begin to match those from the uniform dense test.

It should be noted that some results may have been affected by the proximity of the layer interface to the surface. At the depth of the layer interface ($\approx$ 80mm), the displacements in the uniform dense and loose tests (Figure 2) appear to be affected by the ground surface (not yet reaching a steady trend). Ideally this layer interface would have been located at a deeper location.

Figure 9 presents the $\xi'$ results based on displacements at the other values of lateral offsets ($2\,X/B = 2 \rightarrow 6$). Again, the scatter in $\xi'_{\Delta x}$ is attributed to

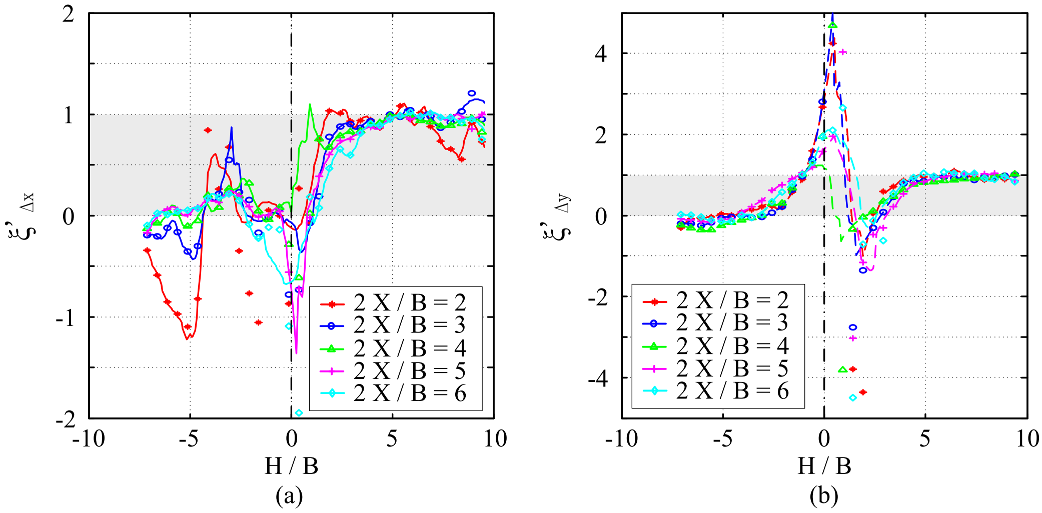


Figure 9: $\xi'$ with variation of offset: $2X/B = 2 \rightarrow 6$ (T04)

the similar horizontal displacement in dense and loose sand. Data smoothing was thus applied by a method of robust local regression in Matlab, using a span of 5 % of the total number of data points. The transition curves of $\xi'_{\Delta x}$ and $\eta'$ seem to show comparable extents of the transition zones around the soil layer interface (i.e. $2B$ in loose sand and $4B$ in dense sand for T04), though the scatter in the loose layer makes delineation of the transition zone difficult. The trend of $\xi'_{\Delta y}$ is relatively clear, with a peak value occurring adjacent to the layer interface, followed by a negative value and then levelling off towards 1. The data suggests that the offset from the penetrometer does not have a significant influence on the trend of $\xi'$.

Figure 10 shows the transition of $\xi'_{\Delta y}$ for all the layered soil tests, including two-layer (subplot a) and three-layer tests (subplot b, where $H_t$ is the thickness of the sandwiched soil layer). Similar to the trends of $\eta'$ in Figure 4, the layered effects are clear, with either a drastic jump or a peak/minimum around the soil layer interfaces. The thin-layer effect (from the three-layer tests in Figure 10b) is shown to cause considerable fluctuations of the $\eta'$ data at the location of the layer interfaces. The dramatic variation of $\xi'_{\Delta y}$ near the first soil layer interface may, like the data presented in Figures 8 and 10a, be due to surface effects. The transition around the second soil layer interface, located at a depth of $\approx$ 150 mm where surface effects on the uniform test data (Figure 2) are insignificant, shows a more reasonable peak at the dense-over-loose interface and a minimum at the loose-over-dense interface. The value of $\xi'_{\Delta y}$ around the dense-over-loose interface for T06 is greater than 1, indicating that the layer interface is moved vertically downwards more than in the uniform sand tests. Correspondingly, the loose-over-dense interface for T06 with $\xi'_{\Delta y} < 0$ indicates that vertical displacements were less than in both of the uniform sand tests, confirming the phenomenon observed from Figure 7.

The distributions of soil deformation around the penetrometer provide insights into the mechanisms that are responsible for the probe resistance data as the cone passes between soil layers. Figure 11 schematically illustrates the displacement mechanisms for penetration in layered soils. For soil above a loose-over-dense interface, the vertical displacements are restricted by the underlying stiffer layer with lower compressibility. For the dense-over-loose interface, larger vertical displacements occur owing to the cumulative densification of the underlying, more compressible layer. Although test results were somewhat affected by the proximity of the ground surface to some of the layer interfaces, the effects of soil layering on trends of displacements

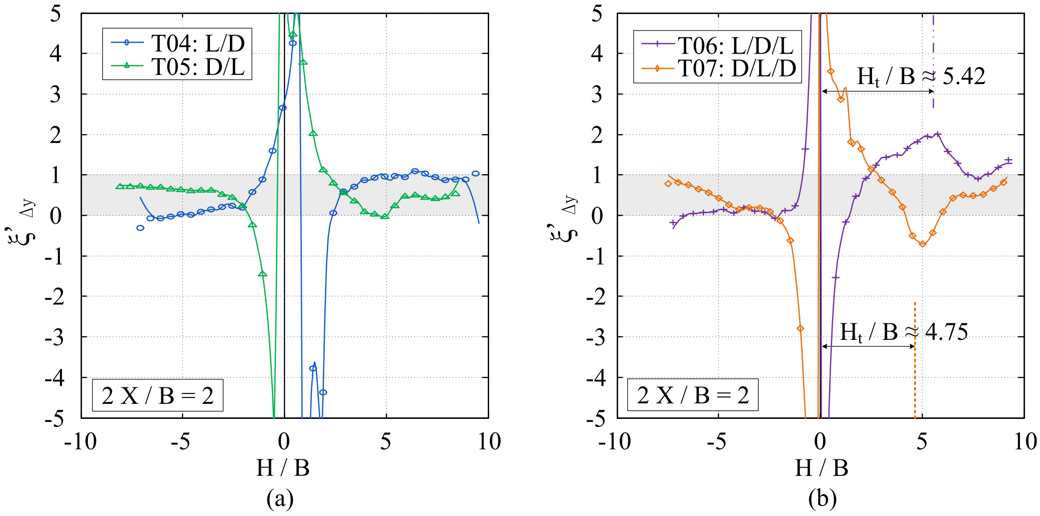


Figure 10: Layered effects on soil deformation ($2\,X/B = 2$) for tests with: (a) two-layered soils; and (b) three-layered soils

was generally clear. The observations provided in this paper may assist in the qualitative interpretation of CPT data; further work is still required to achieve a quantitative methodology for relating penetration resistance and soil deformations in layered soils. The results provided here may also provide a useful validation dataset for new developments of numerical and analytical methods for CPT data interpretation.

## 4. Conclusions

This paper presented data obtained from a series of centrifuge tests aimed at investigating the effects of soil layering on ground displacement mechanisms around the probe.

Data from uniform soil tests was provided as a reference to compare layered test data against. The effects of soil density and stress level were

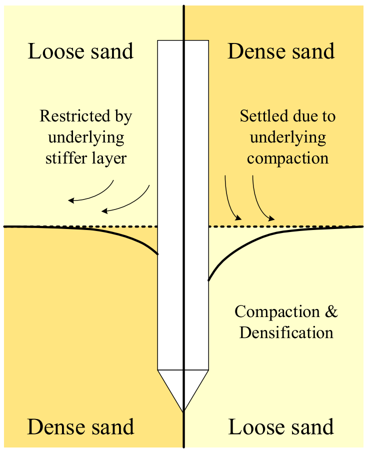


Figure 11: Schematic of displacement mechanism for penetration in layered soils

illustrated from the uniform test results. A large influence zone based on soil displacements was noted for the dense sand, owing to its relatively low compressibility. The large influence zone and associated higher soil stresses relates well to higher penetration resistance in the dense soil compared to the loose soil. A larger deformation zone was observed under lower stress conditions due to the increased tendency of the soil to dilate. This results in a relatively high stress state around the probe under low stress conditions, which explains the non-linear increase of penetration resistance with stress level.

Soil layering was shown to have a clear effect on soil deformation patterns. The change of vertical displacement profile around the soil layer interfaces was more obvious than for the horizontal displacement profile. A peak value of soil vertical displacement occurred at dense-over-loose interfaces, while a local minimum occurred at loose-over-dense interfaces. Additionally, displacements at loose-over-dense interfaces were less than those that occurred in both the uniform dense and loose tests. For the dense-over-loose interfaces, the displacements were greater than for the uniform soil tests.

The parameters $\xi'_{\Delta x}$ and $\xi'_{\Delta y}$ were proposed to evaluate the transition of displacement profiles for penetration in layered soils. The trends of $\xi'$ provided a quantitative evaluation of the layered effects on soil deformation. The transition curves of $\xi'_{\Delta x}$ and $\eta'$ were noted to be comparable, with similar extents of transition zones around the soil layer interface, though the scatter in the $\xi'_{\Delta x}$ made conclusive delineation of transition zones difficult. The trend of $\xi'_{\Delta y}$ was relatively clear, with a peak value occurring adjacent to the dense-over-loose interface and a minimum at the loose-over-dense interface. It was shown that the offset distance from the pile did not significantly affect the profile of $\xi'$. A deformation mechanism for penetration in layered soils was described based on the observed results from the centrifuge tests.

## 5. Acknowledgments

The authors would like to acknowledge financial support by the Fundamental Research Funds for the Central Universities (No. 2017QNB10).

## References

Ahmadi, M. M., Robertson, P. K., 2005. Thin-layer effects on the CPT q(c) measurement. Canadian Geotechnical Journal 42 (5), 1302–1317.

Bolton, M. D., Gui, M. W., Garnier, J., Corte, J. F., Bagge, G., Laue, J., Renzi, R., 1999. Centrifuge cone penetration tests in sand. Géotechnique 49 (4), 543–552.

Gui, M., Bolton, M. D., 1998. Geometry and scale effect in cpt and pile design. In: Robertson, P., Mayne, P. (Eds.), Geotechnical Site Characterization: Proceedings of the First International Conference on Site Characterization, ISC'98. Vol. 2. Balkema, Rotterdam, Atlanta, Georgia, pp. 1063–1068.

Jamiolkowski, M., Ghionna, V. N., Lancellotta, R., Pasqualini, E., 1988. New correlations of penetration test for design practice. Invited Lecture. In: ISOPT-1. pp. 196–263.

Lee, S. Y., 1990. Centrifuge modelling of cone penetration testing in cohesionless soils. Ph.D. thesis, University of Cambridge, UK.

Liu, W., 2010. Axismmetric centrifuge modelling of deep penetration in sand. Ph.D. thesis, University of Nottingham.

Meyerhof, G. G., Sastry, V. V. R. N., 1978a. Bearing capacity of piles in layered soils.1. clay overlying sand. Canadian Geotechnical Journal 15 (2), 171–182.

Meyerhof, G. G., Sastry, V. V. R. N., 1978b. Bearing capacity of piles in layered soils.2. sand overlying clay. Canadian Geotechnical Journal 15 (2), 183–189.

Mo, P. Q., 2014. Centrifuge modelling and analytical solutions for the cone penetration test in layered soil. Ph.D. thesis, University of Nottingham.

Mo, P. Q., Marshall, A. M., Yu, H. S., 2015. Centrifuge modelling of cone penetration tests in layered soils. Géotechnique 65 (6), 468–481.

Mo, P. Q., Marshall, A. M., Yu, H. S., 2017. Interpretation of cone penetration test data in layered soils using cavity expansion analysis. Journal of Geotechnical and Geoenvironmental Engineering 143 (1), 04016084–1–12. DOI: 10.1061/(ASCE)GT.1943–5606.0001577.

Paniagua, P., Ando, E., Silva, M., Emdal, A., Nordal, S., Viggiani, G., 2013. Soil deformation around a penetrating cone in silt. Géotechnique Letters 3, 185–191.

Sadrekarimi, A., 2016. Evaluation of cpt-based characterization methods for loose to medium-dense sands. Soils and Foundations 56 (3), 460–472.

Vreugdenhil, R., Davis, R., Berrill, J., 1994. Interpretation of cone penetration results in multilayered soils. International Journal for Numerical and Analytical Methods in Geomechanics 18 (9), 585–599.

Walker, J., Yu, H. S., 2010. Analysis of the cone penetration test in layered clay. Géotechnique 60 (12), 939–948.

White, D. J., 2002. An investigation into the behaviour of pressed-in piles. Ph.D. thesis, Cambridge University.

White, D. J., Bolton, M. D., 2004. Displacement and strain paths during plane-strain model pile installation in sand. Géotechnique 54 (6), 375–397.

White, D. J., Take, W. A., Bolton, M. D., 2003. Soil deformation measurement using particle image velocimetry (PIV) and photogrammetry. Géotechnique 53 (7).

Xu, X. T., 2007. Investigation of the end bearing performance of displacement piles in sand. Ph.D. thesis, The University of Western Australia.

Xu, X. T., Lehane, B. M., 2008. Pile and penetrometer end bearing resistance in two-layered soil profiles. Géotechnique 58 (3), 187–197.

Youd, T. L., Idriss, I. M., 2001. Liquefaction resistance of soils: Summary report from the 1996 NCEER and 1998 NCEER/NSF workshops on evaluation of liquefaction resistance of soils. Journal of Geotechnical and Geoenvironmental Engineering 127 (4), 297–313.